ACS MATERIALS Au
AN OPEN ACCESS JOURNAL OF THE AMERICAN CHEMICAL SOCIETY

pubs.acs.org/materialsau

Article

# How Ionic Liquid Gels Work on the Removal of Bisphenol A from Wastewater

Salvatore Marullo and Francesca D'Anna*

Cite This: *ACS Mater. Au* 2023, 3, 112–122

Read Online

ACCESS | Metrics & More | Article Recommendations | Supporting Information

**ABSTRACT:** The occurrence of emerging pollutants in water bodies is a pressing issue of modern society and identifying materials to remove them is the main target of current research. In this work, we prepared and characterized supramolecular gels of 1,3:2,4-dibenzylidene-D-sorbitol (DBS) in ionic liquids differing for the anion and the aliphatic or aromatic nature of the cation. We characterized our gels for their thermal stability and mechanical properties. We also found that all gels self-heal in 24 h after being cut by a razor blade. We then used our gels as sorbents to remove bisphenol A, an endocrine disruptor compound, from aqueous solutions. All gels adsorb BPA with high removal efficiencies, and those obtained in aliphatic ionic liquids act faster than their aromatic counterparts. The highest observed adsorption capacity was 314 mg/g. Gels were reused without loss in performance and need for intermediate washing, and the gel obtained in [bmpip][$NTf_2$] could be reused 37 times, maintaining a removal efficiency higher than 96%. It was loaded in a sequential system of syringes to treat flowing aqueous phases, removing 60% of BPA in 30 min. We also embedded the gel in the dialysis membrane and observed a removal efficiency of 85% after 48 h.

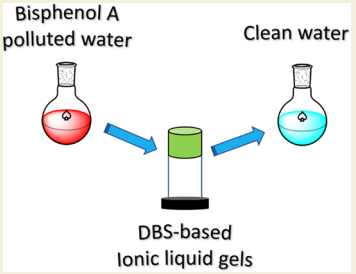


**KEYWORDS:** *emergent pollutants, adsorption, supramolecular gels, BPA, ionic liquids*

## INTRODUCTION

Tackling pollution of water bodies is a problem of prominent importance in present-day society, given the importance of such limited resources. As a result, the occurrence and concentration of many compounds in water are strictly regulated by law. However, in recent years, a further issue raises concerns, such as the increasing presence in urban wastewater of compounds for which, in many cases, regulations do not yet exist.[1] These compounds are known as emerging pollutants (EPs) and span a wide range of classes and structures.[2] In particular, some frequently encountered categories include pharmaceutically active compounds such as antibiotics or anti-inflammatory drugs, disinfectants, personal care products, plastic additives, and plasticizers.[3] A group of EPs is one of the endocrine disruptor compounds (EDCs), which are known to interfere with the endocrine system of humans and animals,[4,5] and among these, a compound like bisphenol A (BPA) raises particular concern.

BPA is mainly used in the production of plastic materials such as polycarbonates and epoxy resins,[6] and the exposure to this compound has been linked to adverse effects such as neurotoxicity, obesity, and xenoestrogen activity.[7] Consequently, different methods have been developed to remove BPA from water bodies. To this aim, commonly used methods for BPA removal include advanced oxidation processes, membrane filtration, and biological methods.[8] Recently, adsorption methods have risen to some prominence[9,10] due to their convenient characteristics, such as the simplicity of use, the relatively low energy consumption, their cost-effectiveness, and, in many cases, high removal efficiency.[11] In this respect, commonly used sorbents for BPA removal include zeolites,[12] agricultural waste,[13,14] and polysaccharides such as chitosan.[15,16] In recent years, a remarkable interest has been laid in the use of nanostructured sorbents, owing to their high surface area, coupled in several cases with a high uptake of pollutants and selectivity.[17] Examples of nanostructured sorbents for the treatment of wastewater include metal−organic frameworks,[18] graphene oxide,[19] and supramolecular gels.[20] Supramolecular gels are soft materials resulting from the self-assembly of molecules known as low-molecular-weight gelators (LMWGs) which, in dilute solutions, form a sample-spanning network able to entrap high amounts of the solvent.[21,22] Consequently, the resulting material has a solid-like appearance despite being constituted prominently by the solvent and is underpinned solely by noncovalent interactions. When used as sorbents, gels often prove to be efficient and robust sorbents toward a wide range of pollutants owing to their high surface area exposed to the polluted water and the high mechanical resistance, allowing the gel to be reused for several cycles without breaking. Although supramolecular gels have been successfully employed for the sequestration of many types of pollutants, they have

Received: September 30, 2022
Revised: November 12, 2022
Accepted: November 14, 2022
Published: November 29, 2022

© 2022 The Authors. Published by American Chemical Society

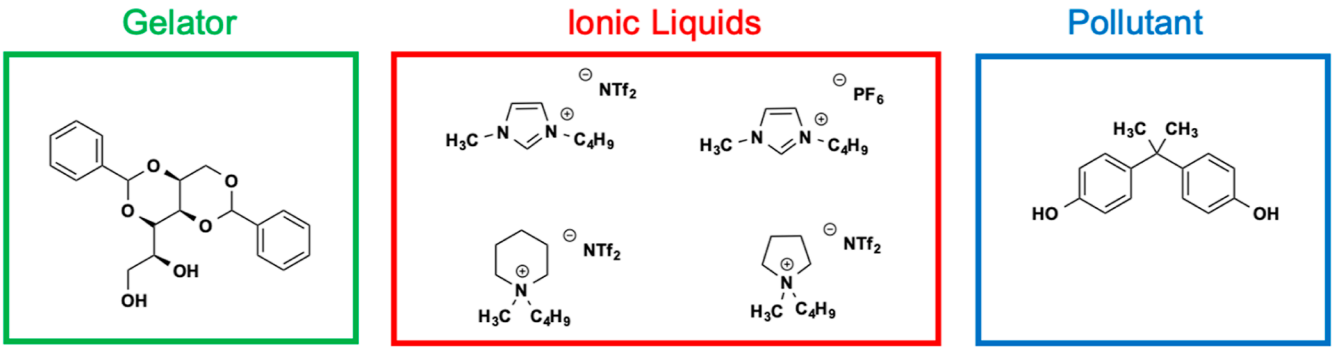


**Figure 1.** Structures of the gelator, ionic liquids, and pollutant employed.

been largely overlooked for the removal of BPA. In this regard, most gel-based systems for adsorbing BPA reported in the literature feature polymer gels, which are underpinned by covalent bonds resulting from the cross-linking of polymer chains. In particular, these include xanthan gum-,[23] polycyclodextrin,-[24,25] or imidazolium-functionalized-based polymer hydrogels.[26] In the framework of our interest in investigating the properties of gels in nonconventional solvents, we found that supramolecular gels in ionic liquids (ILs), known as IL gels (ILGs), can be successfully employed to remove a wide range of pollutants from both organic solvents and water, spanning from sulfur compounds in fuels,[27,28] to dyes[29] and pharmaceutically active compounds from aqueous solutions.[30] Based on these considerations, we prepared and characterized ILGs obtained from DBS in ionic liquids (Figure 1).

DBS is a well-known gelator for organic solvents,[31] and recently, it has also been reported that it can harden deep eutectic solvents.[32]

We chose ionic liquids differing for the anion and the aromatic or aliphatic nature of the cation. The gels obtained were characterized for their thermal stability and morphology by SEM images, as well as their rheology by sweep and frequency sweep measurements. The ILGs were then used to remove BPA from aqueous solutions. The gels showed a high removal efficiency along with good to high recyclability. In particular, the best-performing one was reused 37 times with negligible loss in performance. This gel is resistant enough to be used for loading in columns for the sequential decontamination of flowing aqueous phases or embedded in dialysis membranes for the treatment of larger volumes of polluted waters.

## MATERIALS AND METHODS

### Materials

Acetone, maleic acid, bisphenol A, rhodamine B, ethyl acetate, methanol, ethanol, toluene, 2-methyltetrahydrofuran, and diethyleneglycol dimethylether were purchased and used without further purification. Commercially available 1-butyl-3-methyl-imidazolium hexafluorophosphate ([bmim][$PF_6$]), 1-butyl-3-methyl-imidazolium bis-(trifluoromethanesulfonyl)imide ([bmim][$NTf_2$]), 1-butyl-1-methylpyrrolidinium bis-(trifluoromethanesulfonyl)imide ([bmpyrr][$NTf_2$]), and 1-butyl-1-methylpiperidinium bis-(trifluoromethanesulfonyl)imide ([bmpip][$NTf_2$]) were dried at 60 °C under reduced pressure and kept in a desiccator under argon before use.

### 1,3:2,4-Dibenzylidene-D-sorbitol (DBS)

1,3:2,4-Dibenzylidene-D-sorbitol was synthesized according to a published procedure.[33]

### Gelation Tests

In a screw-capped vial, suitable amounts of DBS and ILs were weighed and heated at 80 °C for 1 h to obtain a clear solution. Subsequently, the solution was kept at 4 °C overnight. Gel formation was assessed by the tube inversion test.[34]

### $T_{gel}$ Determination

$T_{gel}$ were determined by the falling drop method.[35] A vial containing the preformed gel was placed upside-down in a water bath. The bath temperature was raised gradually (1 °C/min) until the gel collapsed and flow was observed. $T_{gel}$ values were reproducible within 1 °C.

### Rheology Measurements

Rheological measurements were carried out using a strain-controlled rheometer using a Peltier temperature controller and a plate−plate tool. For a typical measurement, the preformed gel was placed between the shearing plates of the rheometer. Strain and frequency sweep measurements were carried out at 25 °C on three different aliquots of gels.

### SEM Images

SEM measurements were carried out using a PRO X PHENOM electronic scanning microscope, operating at 5 kV. Xerogels for each sample were obtained by placing each gel on an aluminum stub and then washing it with ethanol to remove the IL, following a previously reported procedure.[36,37]

### Thixotropy and Sonotropy Tests

To evaluate thixotropic behavior, a magnetic stir bar was placed on top of the gel and stirred for 5 min at 400 rpm. Whenever the gel was broken, it was kept at 4 °C overnight to verify if the gel was restored. For sonotropy tests, each gel was subjected to sonication for 5 min, using an ultrasonic bath operating at 45 kHz with an output power of 200 W. The restoration of the gel was checked as previously described.

### Swelling and Porosity

The porosity and swelling of all ILGs were determined according to reported procedures[28,38,39] using hexane as the solvent. Hexane was cast on gels for 24 h. By knowing the initial weight of the empty vial ($W_1$), the weight of the vial and the gel before ($W_{dry}$) and after ($W_2$) adding hexane and the final weight of the vial and gel after removing hexane ($W_3 = W_{wet}$), it was possible to determine the porosity ($P$) and swelling ($Q$) using the following equations

$$V_g = 4 - \left(\frac{W_2 - W_1 - W_{dry}}{\rho_h}\right) \quad (1)$$

$$V_p = \frac{W_2 - W_3 - W_{dry}}{\rho_h} \quad (2)$$

$$P = \frac{V_p}{V_p + V_g} \times 100 \quad (3)$$



https://doi.org/10.1021/acsmaterialsau.2c00066
ACS Mater. Au 2023, 3, 112−122

$$Q = \frac{W_{wet} - W_{dry}}{W_{dry}} \times 100 \quad (4)$$

where $\rho_h$ is the density of hexane and $V_g$ and $V_p$ (mL) represent the volume of gel and hexane in the pores, respectively. 4 mL is the total volume occupied by the gel and hexane.

### BPA Removal Tests

Aqueous solutions of BPA were prepared by the dilution of stock solutions of BPA in methanol. The latter was diluted in water to achieve the desired concentration by maintaining the amount of methanol at 1% v/v. BPA adsorption tests were carried out in vials by placing it onto 250 mg of preformed gel (3 wt %) and 500 $\mu$L of a $4 \times 10^{-4}$ M BPA aqueous solution. After a given time, an aliquot of the solution was withdrawn and suitably diluted, and then the relevant UV spectrum was recorded. The residual concentration of BPA was determined based on a calibration curve previously determined. For concentration-dependent measurements, 250 mg of the preformed gel was put in contact with 20 mL of solutions of BPA at variable concentrations for 24 h. From these experiments, the equilibrium adsorption capacity $Q_e$ was determined using eq 5

$$Q_e = \frac{(C_0 - C_e)V}{m} \quad (5)$$

where $C_0$ is the initial concentration of BPA and $C_e$ is the equilibrium concentration of BPA expressed in mg/mL. Furthermore, $m$ is the mass in mg of the gel and $V$ is the volume of solution, expressed in mL.

Gel recycling experiments were carried out by removing the aqueous phase after an adsorption run and replacing it with a fresh batch of BPA solution. The residual concentration of BPA was determined as described above.

Sequential adsorption tests were carried out as described in the literature.[29] To this aim, 500 mg of gel was introduced into a 1 mL syringe with a filter paper disk at the bottom of the syringe. Then, 1 mL of the aqueous solution was added from the top of the column. An outflow of solution bottom of the syringe was observed and introduced in the next syringe filled with another aliquot of gel. This procedure was repeated a third time. The experiment was performed in triplicate under atmospheric pressure and at room temperature.

Adsorption tests with the gel embedded in the dialysis membrane were conducted following a reported procedure.[30]

## RESULTS AND DISCUSSION

### Gelation Tests

Gels of DBS in ionic liquids were prepared by heating mixtures of DBS and IL at 80 °C until complete dissolution. Then, the mixture was kept at 4 °C overnight. Gel formation was assessed by the tube inversion test.[40] With all the ionic liquids considered, we obtained opaque gels. The minimum amount of DBS able to yield a gel, known as critical gelation concentration (CGG), was also determined, obtaining the results reported in Table 1.

Looking at the results reported in Table 1, it is found that CGC is very similar in all ILs, with no particular effect exerted by the aromatic or aliphatic nature of the cation, as well as by the nature of the anion. Then, we determined the gel−sol transition temperature, at the common gelator concentration of 3 wt %, by the falling drop method,[35] obtaining the results reported in Table 1. The latter show that the IL has a significant effect on the thermal stability of the gel, with $T_{gel}$ increasing along the sequence [bmim][$NTf_2$] < [bmpip][$NTf_2$] ≈ [bmim][$PF_6$] < [bmpyrr][$NTf_2$]. Dissecting the effect of IL cation or anion reveals that ILs with aliphatic cations, such as [$bmpip^+$] and [$bmpyrr^+$], give rise to the most thermally stable gels. On the other hand, changing the anion from [$NTf_2^-$] to [$PF_6^-$] has a more marginal effect, with a slightly higher $T_{gel}$ in the IL bearing the more symmetrical and more cross-linking [$PF_6^-$]. Differently from what we observed in ionic liquid gels formed by organic salts,[41] the hydrogen bonding accepting ability anion, as expressed by the Kamlet−Taft $\beta$ parameter, does not dominate the anion effect, given that $T_{gel}$s are nearly identical for the two ILs ($\beta$ = 0.21 and 0.24 for [bmim][$NTf_2$] and [bmim][$PF_6$], respectively).[42]

**Table 1. Critical Gelation Concentrations (CGC) and $T_{gel}$ at 3 wt % for DBS-Based ILGs**

| ionic liquid | CGC (wt %) | $T_{gel}$ at 3 wt % (°C) |
|---|---|---|
| [bmim][$PF_6$] | 2.0 | 70 |
| [bmim][$NTf_2$] | 3.0 | 65 |
| [bmpip][$NTf_2$] | 3.0 | 69 |
| [bmpyrr][$NTf_2$] | 2.0 | 80 |

### Rheology

To gain information on the mechanical properties of the gels, we carried out rheological measurements such as strain and frequency sweeps. In such measurements, the storage modulus ($G'$) and the loss modulus ($G''$) are measured as a function of the strain applied or the frequency applied. As a result, parameters such as $G'$ and $G''$ can be extracted, which account for the solid- or liquid-like rheological response, respectively. Moreover, information on the mechanical strength is provided by the strain at the crossover point ($\gamma_c$) or the tan $\delta$ which is related to the strength of colloidal forces underpinning the gel network. Representative plots obtained in these measurements are reported in Figure 2, while the others are shown in Figure S1 of the Supporting Information. From these measurements, we determined the rheological parameters reported in Table 2.

An examination of the rheological parameters reported in Table 2 shows the dominance of solid-like behavior of all ionogels, as shown by the values of tan ($\delta$), much lower than unity, suggestive of strong interactions within the gel network.[43] However, looking at the other parameters, a clear distinction between the properties of gels obtained in ILs with aliphatic or aromatic cations can be made. In particular, the latter, namely, the gels in [bmim][$NTf_2$] and [bmim][$PF_6$], have higher mechanical resistance, as shown by the much higher values of the strain at the crossover point ($\gamma_c$), that is, the strain required to break down the gel. On the other hand, the gels obtained in aliphatic ILs, [bmpyrr][$NTf_2$] and [bmpip][$NTf_2$], are mechanically weaker, with this latter being able to withstand a rather limited strain. Further examination of the rheological results reveals an inverse relationship between the stiffness of the gels, expressed by the storage modulus, $G'$, and the mechanical strength, expressed as $\gamma_c$.

In particular, the gels obtained in aliphatic ILs show much higher values of $G'$, compared with their aromatic counterpart, which, as already said, are able to withstand higher mechanical strains. These findings show the occurrence of a more rigid gel network in the presence of aliphatic ILs, giving rise to more brittle materials, which break more easily. Conversely, the gels obtained in aromatic ILs are more flexible and on balance more resistant to mechanical strain. Finally, comparing the rheological parameters determined for [bmim][$NTf_2$] and [bmim][$PF_6$] shows that the IL anion does not exert a significant influence, given that the values obtained for the two gels are practically comparable. We propose that the higher


https://doi.org/10.1021/acsmaterialsau.2c00066
ACS Mater. Au 2023, 3, 112−122

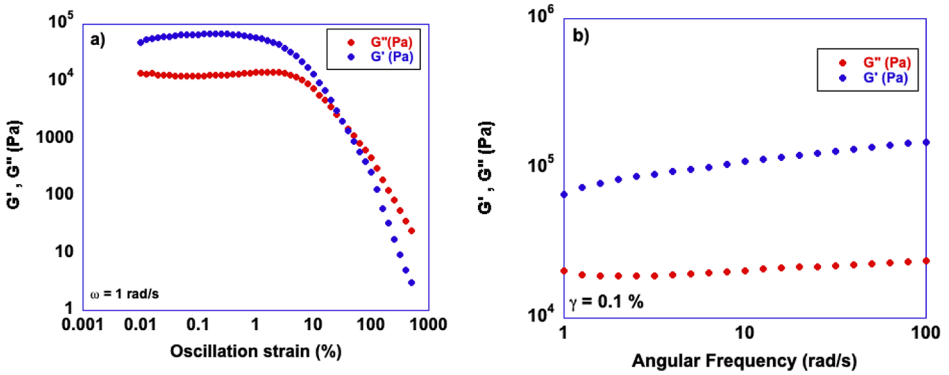


**Figure 2.** Plots of (a) strain sweep and (b) frequency sweep measurement for the 3 wt % DBS-based gel in [bmpyrr][$NTf_2$], at 25 °C.

**Table 2. Rheological Parameters for DBS-Based Ionic Liquid Gels at 25 °C**

| IL | $G'$ (Pa) | $G''$ (Pa) | tan ($\delta$) | $\gamma_c$ at $G' = G''$ (%) |
|---|---|---|---|---|
| [bmpyrr][$NTf_2$] | 85,000 ± 20,000 | 19,000 ± 5000 | 0.23 ± 0.07 | 32 ± 8 |
| [bmim][$NTf_2$] | 7000 ± 2000 | 1400 ± 180 | 0.21 ± 0.06 | 140 ± 20 |
| [bmim][$PF_6$] | 9000 ± 3000 | 1800 ± 600 | 0.23 ± 0.04 | 125 ± 30 |
| [bmpip][$NTf_2$] | 40,000 ± 16,000 | 10,000 ± 2000 | 0.23 ± 0.03 | 1.8 ± 0.3 |

flexibility of the gels obtained in aromatic ILs may derive from the $\pi-\pi$ interactions between the phenyl rings of DBS and the aromatic cations of the IL. In particular, these feeble interactions, which can be broken and reformed more easily than ion−dipole interactions, may allow the gelator to "slide" within the gel network under shear, without breaking it. Conversely, in the aliphatic IL-based gels, the gelator is less free and held more tightly in the gel network by hydrogen bonding and ion−dipole interactions, yielding an overall more rigid gel.

## Self-Healing Ability

We then investigated if our ILGs show thixotropic or sonotropic behavior, that is, if they spontaneously reform after being broken by mechanical stress or after being subjected to sonication. To assess thixotropy, we put a magnetic stirring bar on top of each gel (250 mg, 3 wt %) and then subjected it to stirring at 400 rpm for 15 min. In the other case, each gel was sonicated in an ultrasound bath (45 kHz, 200 W) for 5 min. In both instances, when a gel was broken as a result of the treatment, we kept it at 4 °C overnight. Subsequently, we verified if the gel was restored by the tube inversion test. The results obtained showed that all ionic liquid gels are stable to both stimuli, mechanical and ultrasonic. This agrees with the results collected by the rheological measurements. It is worth noting that the same stimuli are strong enough to break other supramolecular ILGs reported in the literature.[27,29,44] Encouraged by these results, we went on to probe the self-healing ability of our gels. To this aim, we prepared two identical gels, staining one of them with 0.25 wt % of the dye rhodamine B. Then, we cut each gel in half with a razor blade and put into contact the pristine gel half with the stained gel one. A pictorial representation of the procedure followed is reported in Figure 3.

Subsequently, we monitored the appearance of the two halves into contact, over time. Representative pictures taken for the gel obtained in [bmpyrr][$NTf_2$] (3 wt %) are reported in Figure 4, while the ones relevant to the other gels are reported in Figure S2.

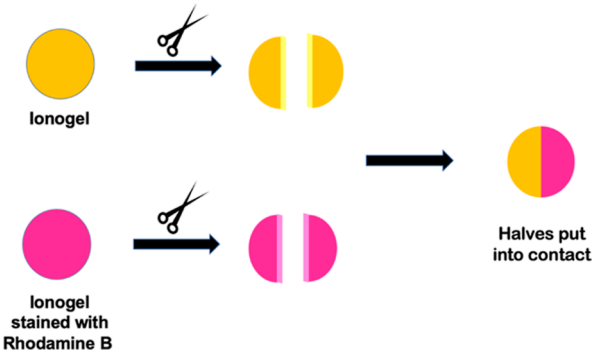


**Figure 3.** Pictorial schematic representation of the procedure followed to assess the self-healing ability of the gels.

Looking at the pictures reported in Figure 4, we can appreciate that after 5 h, the dye starts to diffuse through the other half of the ILGs, suggesting partial healing of the material. After 24 h, the diffusion of the dye through the healed gel is more evident and involves the entirety of the contact surface. Moreover, from this time on, the two halves behave as a single gel, and the newly healed gel is self-supporting, as assessed by the inversion test. A similar conclusion can be drawn for the other gels by looking at the pictures reported in Figure S2. The inversion test gave a positive response for the other gels alike after 24 h, therefore confirming the good self-healing ability of the DBS-based gels.

## Morphology

To gain information about the morphology of our gels, we recorded SEM images of the relevant xerogels, obtained by washing the gels with ethanol, to remove the ILs, following a reported procedure.[45] We are aware that obtaining xerogels may lead to a change in the size of the structures being imaged. This is why we use SEM only for a qualitative comparison. The images obtained for the ILGs at 3 wt % are reported in Figure 5.

Looking at the SEM images reported in Figure 5, it is found that the DBS-based ILGs have different morphologies depending on the ionic liquid used. In particular, the gel


https://doi.org/10.1021/acsmaterialsau.2c00066
ACS Mater. Au 2023, 3, 112−122

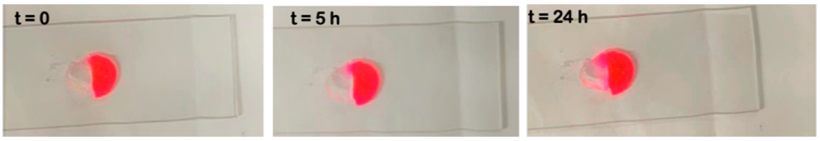


**Figure 4.** Pictures of the cut halves of the gel of DBS in [bmpyrr][$NTf_2$] (3 wt %) taken at different times.

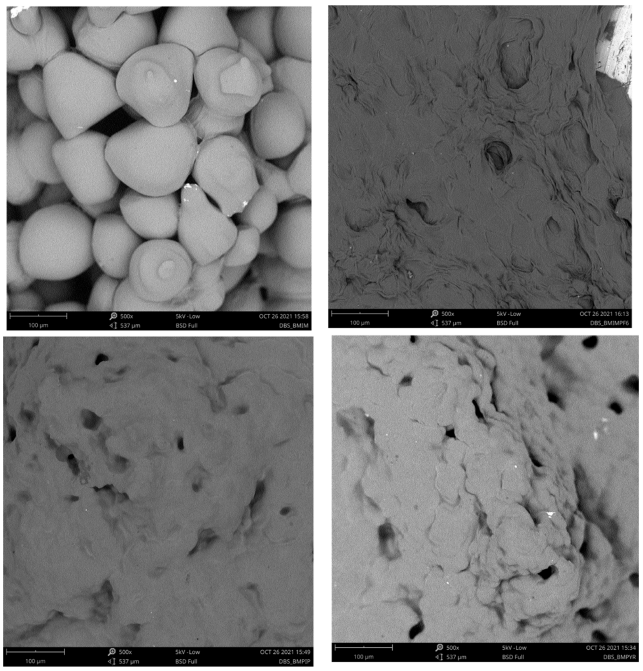

**Figure 5.** SEM images of the xerogels relevant to DBS-based ILGs (3 wt %) in the top left [bmim][$NTf_2$], top right [bmim][$PF_6$], bottom left [bmpip][$NTf_2$], and bottom right [bmpyrr][$NTf_2$].

obtained in [bmim][$NTf_2$] exhibits a distinct morphology characterized by the occurrence of spheroidal structures uniformly distributed over the sample. A very different picture emerges for the gels in the other ILs, for which it is difficult to extract an obvious morphology. Instead, a very thick and compact texture is found with the occurrence of pores throughout the samples.

## Porosity and Swelling

The porosity of a gel is an important property when the gel phase is used to trap pollutants via adsorption. For this reason, we estimated the porosity and swelling of our ionic liquid gels, using the reported procedures.[28,38] These parameters are determined by letting the gel make contact with a solvent. Moreover, in particular, swelling is defined as the increase in mass of the gel, as a consequence of contact with the solvent. This parameter, together with the known density of the solvent, allows us to determine the porosity of the gel, which is defined as the ratio between the total volume occupied by pores and the volume of the gel. It is worth noting that a suitable solvent for the reliable determination of gel porosity should induce minimal or negligible swelling so that the porosity being measured is the one of the pristine gel and not one of the gels swollen by the solvent. The solvent chosen for this determination is *n*-hexane, which was kept in contact with the gel for 24 h at 25 °C. We could not determine the porosity of the gel in [bmim][$NTf_2$] due to its partial dissolution upon contact with hexane.

Experimental details and equations defining these parameters are reported in the Materials and Methods section, while the results obtained are reported in Table 3.

**Table 3. Swelling and Porosity of IL Gels (3 wt %) Measured after Contact with Hexane at 25 °C for 24 h**

| IL | swelling (%) | porosity (%) |
|---|---|---|
| [bmpyrr][$NTf_2$] | 5 | 94 |
| [bmpip][$NTf_2$] | 19 | 89 |
| [bmim][$PF_6$] | 14 | 52 |

An examination of the results reported in Table 3 shows a negligible to the low entity of swelling in all the gels considered. Furthermore, swelling values increase along the order [bmpyrr][$NTf_2$] < [bmim][$PF_6$] ≈ [bmpip][$NTf_2$]. Looking at gels obtained in aliphatic ILs, a sharp increase in swelling is detected upon going from ILs bearing the pyrrolidinium cation to the one bearing the piperidinium one. This appears to reflect the different conformational freedom of the cations as we move from the more rigid pyrrolidinium to the more flexible piperidinium. Interestingly, this is consistent with the stiffness of the gels as expressed by the storage modulus $G'$ (Table 1), which indicates that the gel in [bmpyrr][$NTf_2$] is the stiffest one. Hence, the lowest swelling confirms that this gel is characterized by a more rigid network, less prone to reorganization upon contact with hexane. In general, the gels obtained in aliphatic ILs show a higher porosity than the ones obtained in the imidazolium IL. On the other hand, no obvious correlation emerges between porosity and the morphology probed by SEM.

## BPA Removal

First, we checked if the gels could withstand the weight of an aqueous phase. To this aim, 500 $\mu$L of water was cast on top of 250 mg of the preformed gel and left in contact for 24 h at 25 °C. In all cases, the gel kept its aspect and was still self-supporting when the vial was inverted. Then, we looked at the possible release of gel components upon contact with water. To this aim, 250 mg of gel (3 wt %) was kept in contact with 500 mg of water for aliphatic IL-based gels and $D_2O$ for the aromatic IL-based ones at 25 °C for 24 h. For the gels obtained in aromatic ILs, we recorded the UV spectrum of the supernatant aqueous phase and determined the amount of IL released based on a previously determined calibration curve. Similarly, for the gels obtained in aliphatic ILs, the $^1$H NMR spectrum of the supernatant aqueous phase was recorded in the presence of a known amount of maleic acid as an internal standard. The results obtained are reported in Table 4.

The results reported in Table 4 show that only a limited release of ILs occurs in the case of the gel in [bmpip][$NTf_2$], amounting to 0.8 wt % of the solvent, whereas in the other case, a minimal or negligible release takes place. In particular, for the aromatic IL-based gels, only 1.0 wt % and 0.3 wt % for [bmim][$NTf_2$] and [bmim][$PF_6$], are released, respectively,


https://doi.org/10.1021/acsmaterialsau.2c00066
ACS Mater. Au 2023, 3, 112−122

**Table 4. Amounts of ILs Released in the Aqueous Phase after 24 h of Contact**

| gel | % IL released |
|---|---|
| DBS in [bmpyrr][$NTf_2$] | |
| DBS in [bmpip][$NTf_2$] | 0.8 |
| DBS in [bmim][$NTf_2$] | 0.3 |
| DBS in [bmim][$PF_6$] | 1.0 |

whereas no significant amount of IL is released by the gel in [bmpyrr][$NTf_2$].

Having verified the stability of the gel upon contact with water, we carried out a static removal test for BPA. To this aim, we put on top of 250 mg of each gel 500 $\mu$L of an aqueous solution of BPA, with a concentration of $4 \times 10^{-4}$ M. At selected times, the supernatant aqueous phase was removed, and its UV-vis spectrum was recorded. The removal efficiency (RE %) was calculated by eq 6

$$\text{RE \%} = \frac{C_i - C_t}{C_i} \times 100 \quad (6)$$

where $C_i$ is the initial concentration of BPA and $C_t$ is the residual concentration of BPA after the time ($t$), based on a calibration curve previously determined. The plots of RE % as a function of time obtained are reported in Figure 6, while the values of RE % observed are reported in Tables S1 and 2.

An examination of the plots reported in Figure 6 shows that, in general, all gels are capable of removing BPA from the solution almost entirely. A closer look reveals an apparent dichotomy between the gels obtained in aromatic and aliphatic ILs. The latter act much faster than their aromatic counterparts, and this can also be seen by comparing the time required to achieve maximum RE %, which amounts to 4 h for the gels in [bmpip][$NTf_2$] and [bmpyrr][$NTf_2$], while 18 h are required for the gel obtained in [bmim][$NTf_2$] and 20 h for the one in [bmim][$PF_6$].

A desirable attribute of a sorbent is its possibility to be reused as much as possible, without the need for intermediate washing. To this aim, we evaluated the possibility of reusing our gels. After an adsorption run, we removed the aqueous phase and replaced it with a fresh batch of BPA solution.

This procedure was repeated until we observed an appreciable reduction in removal efficiency or a drop in the mass of the gel higher than 5%. The results obtained are reported in Figure 7 and Tables S3−5.

The plots reported in Figure 7 clearly show that our gels have good to high degrees of recyclability. In particular, the gel obtained in [bmpyrr][$NTf_2$] can be reused seven times without loss in performance, while the one obtained in [bmim][$PF_6$] maintains its removal efficiency over 12 cycles. Much better results were obtained in the case of the gel in [bmim][$NTf_2$], for which the removal efficiency remained constant over 23 cycles, and the best-performing one was the gel in [bmpip][$NTf_2$], with a high removal efficiency (>96%) maintained over 37 cycles, suffering only a small decrease until the 41st cycle. For the latter gel, we investigated the possibility of recovering BPA from the gel reused 41 times, by letting it make contact with an extraction solvent. In particular, 1 mL of the solvent was cast on top of the gel, which was then stirred for 5 min. Finally, the gel and solvent were kept at 4 °C for 10 min, after which the solvent was removed and diluted in methanol to determine the amount of BPA recovered by spectrophotometry. Among the different solvents used, we obtained the best results with diethylene glycol dimethyl ether, which allowed us to recover 82% of BPA. It is worth noting that after this treatment, the gel was not destroyed.

Subsequently, we carried out a further adsorption run on the regenerated gel to verify its performance after BPA recovery. However, adsorption efficiency steeply dropped to 56%, likely due to some IL being dissolved in the organic phase during the regeneration treatment.

As described above, the gels exhibited a very different recycle performance. In an attempt to elucidate which parameters lead to the highest number of reuse cycles, we compared the trend observed with those of porosity and rheological properties ($G'$ and $\gamma_c$). However, no single parameter can account for the recycling performance observed. For instance, the gels in aliphatic ILs [bmpip][$NTf_2$] and [bmpyrr][$NTf_2$], despite high and comparable porosity, show the best and worst recycling performance, respectively. Similar considerations can be made considering $G'$ or $\gamma_c$. This suggests that the results observed come from the interplay of different factors. In particular, we propose that the highest recycling performance observed for the gel in [bmpip][$NTf_2$] could arise from its concomitant high porosity, high rigidity, and low flexibility, as expressed by the values of $G'$ and $\gamma_c$, respectively. However, given the relatively low number of gels considered, we cannot rule out that other factors come into play.

To obtain further information on the maximum amount of BPA that our gel can remove from aqueous solutions, we

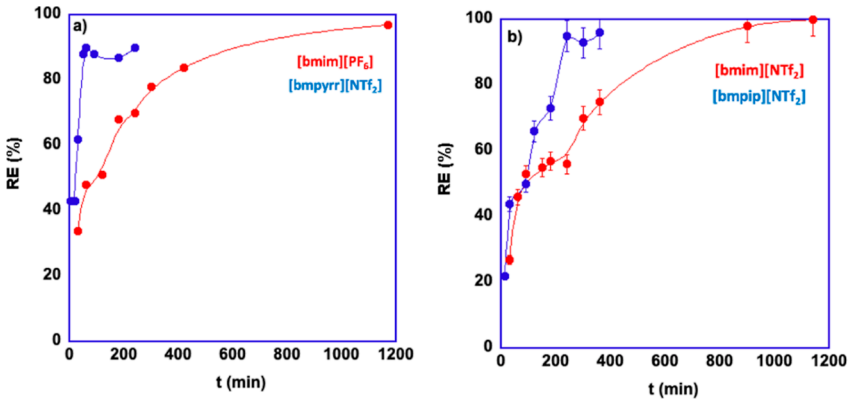


**Figure 6.** Plots of RE % as a function of time for ILGs in contact with the BPA solution at 25 °C for (a) gels in [bmim][$PF_6$] and [bmpyrr][$NTf_2$] and (b) [bmim][$NTf_2$] and [bmpip][$NTf_2$]. Lines are mere visual guides.



https://doi.org/10.1021/acsmaterialsau.2c00066
ACS Mater. Au 2023, 3, 112−122

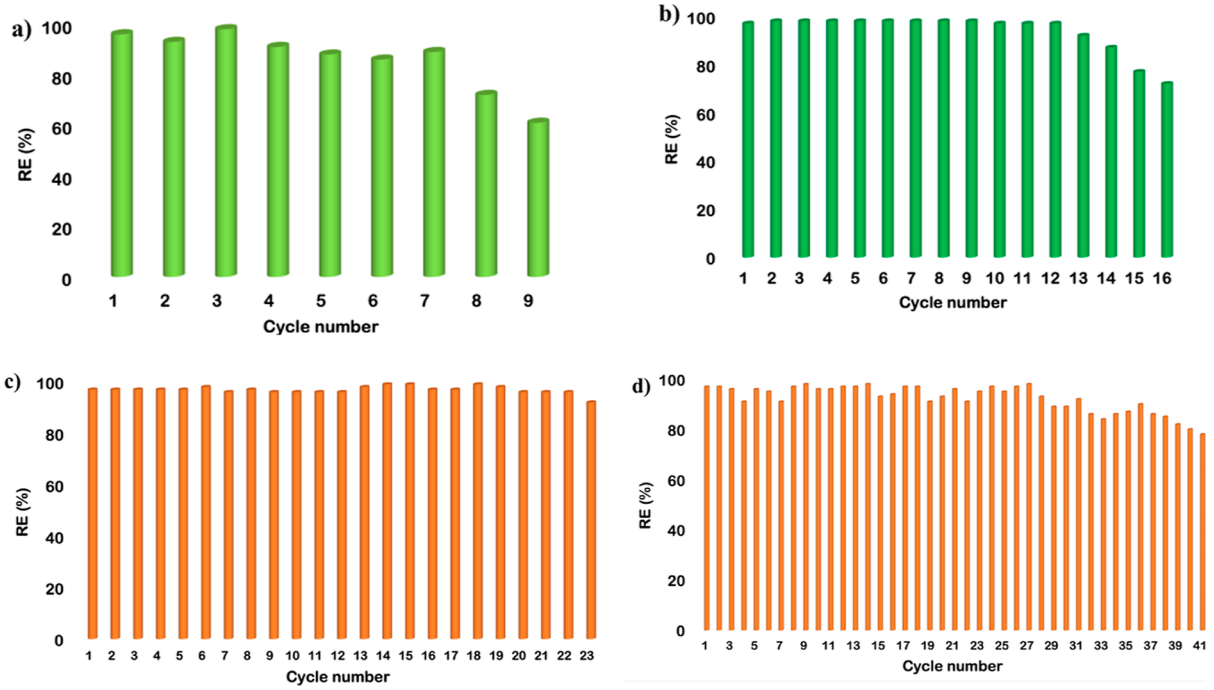


**Figure 7.** Plots of RE % obtained reusing the DBS-based gel obtained in (a) [bmpyrr][$NTf_2$], (b) [bmim][$PF_6$], (c) [bmim][$NTf_2$], and (d) [bmpip][$NTf_2$]. RE % are reproducible within 4%.

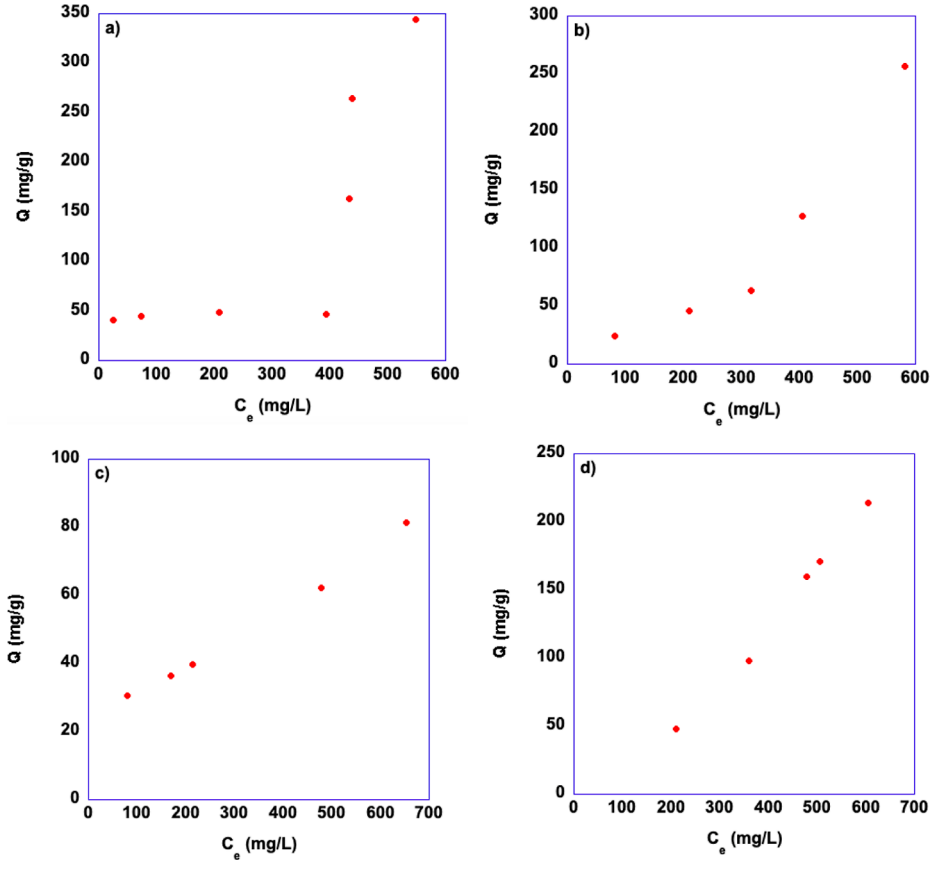


**Figure 8.** Plots of experimental adsorption capacities as a function of initial BPA concentration for 3 wt % gels in (a) [bmim][$NTf_2$], (b) [bmim][$PF_6$], (c) [bmpyrr][$NTf_2$], and (d) [bmpip][$NTf_2$].

carried out adsorption experiments at different concentrations of BPA to determine the maximum amount of BPA that can be adsorbed from the gels. In particular, from each test, we determined the adsorption capacity $Q_c$ by eq 7



https://doi.org/10.1021/acsmaterialsau.2c00066
ACS Mater. Au 2023, 3, 112−122

$$Q_e = \frac{(C_0 - C_e)V}{m} \quad (7)$$

where $C_0$ is the initial concentration of BPA in the solution, $C_e$ is the equilibrium concentration of BPA in the aqueous solution, both expressed in mg/L, $V$ is the volume of the aqueous solution expressed in mL, and $m$ is the mass of gelator expressed in g. The residual concentrations of BPA were determined after 24 h. The results obtained for each gel are reported in Figure 8 and Tables S6 and 7.

Looking at the plots reported in Figure 8, we find a different trend when we compare the result observed for aromatic and aliphatic IL-based gels. It is worth noting that, for these measurements, in all cases, solubility reasons prevented us from reaching the plateau region, so the maximum adsorption capacity of the gels could not be obtained. However, the trend of Q as a function of the initial concentration of BPA shows a linear increase, commonly observed in C- as well as in H- and L-shaped isotherms according to the classification by Giles,[46] at low concentrations. Conversely, the plots relevant to gels obtained in aromatic ILs (Figure 6a,b) suggest that the trend of $Q$ as a function of concentrations follows a sigmoidal, S-shaped isotherm.

This kind of isotherm is less frequently encountered, although it has been observed in the adsorption of some pollutants from water, by different types of sorbents, such as zeolites[47] or silica-based hybrid materials.[48] This kind of trend, has been linked with the occurrence of a cooperative adsorption mechanism[49] or to solute−solute interactions.[47] To the best of our knowledge, this is the first hint of S-shaped isotherms for supramolecular gels.

Regarding the maximum adsorption capacity of our gels, the impossibility of reaching the plateau region allowed us only to determine and measure the highest observed adsorption capacities, which amount to 344 and 260 mg/g for the gels in aromatic ILs, [bmim][$NTf_2$] and [bmim][$PF_6$], respectively, while the highest values determined for the gels in aliphatic ILs were 214 and 81 mg/g for [bmpip][$NTf_2$] and [bmpyrr][$NTf_2$], respectively. Once again, this hints at a difference between the gels in aliphatic or aromatic ILs, with the caveat that these are not $Q_{max}$ values obtained fitting a full isotherm.

Interestingly, the trend of the highest adsorption capacities can be related to the characteristics of the IL entrapped in the three-dimensional network. Indeed, $Q_{max}$ decreases on going from [bmim][$NTf_2$] to [bmim][$PF_6$], parallel to the decrease in the anion coordination ability, as expressed by the Kamlet−Taft parameter $\beta$ ($\beta$ = 0.243 0.207) for [bmim][$NTf_2$] and [bmim][$PF_6$], respectively.[35] On the other hand, with the anion being the same, $Q_{max}$ decreases in parallel with the hydrogen bond donor ability of the cations, expressed by the Kamlet−Taft parameter $\alpha$ ($\alpha$ = 0.617,[42] 0.43,[42] and 0.427[50] for [bmim][$NTf_2$], [bmpip][$NTf_2$], and [bmpyrr][$NTf_2$], respectively). These results suggest that hydrogen bonding is the leading interaction involved in the adsorption process. Consequently, a gel in a solvent more capable of forming hydrogen bonds will be able to adsorb a larger amount of BPA. This finding is consistent with the good performance of diethylenedimethyl ether in recovering BPA from the spent gel. Indeed, according to its hydrogen bond-accepting ability, it can interfere and compete with the adsorption sites within the gel. We previously observed such competitive action in regenerating biobased polymer gels used to remove sulfur compounds from fuels.[28]

After examining the performance of our gels under static adsorption conditions, we moved to investigate their ability to remove BPA from flowing aqueous phases. To this aim, we used the gels as loading for syringes, a BPA aqueous solution ($4 \times 10^{-4}$ M) was allowed to flow through the gel, and the ensuing solution was treated sequentially in the same way two other times. A representative picture of the experimental setup is reported in Figure 9.

**Figure 9.** Picture of gel-loaded syringes for sequential adsorption of BPA form flowing aqueous phases.

In particular, in these adsorption runs, 1 mL of the aqueous solution was allowed to flow through 500 mg of gel. It is worth noting that, to hold the gel in place and prevent it from leaking out from the syringe, we placed a disk of filter paper under the gel. Therefore, we preliminarily checked if the paper disk alone could adsorb BPA. The paper disk adsorbed an amount of BPA equal to 10%. We considered this contribution in the sequential adsorption of BPA over the gel to find the neat removal efficiency. By eluting the BPA aqueous solution onto the gel, we obtained removal efficiencies equal to 49, 83, and 96% after elution on the first, second, and third syringes respectively. Subtracting the contribution of the paper disk, which is assumed constant in all three elutions, we find a removal efficiency of 60%, which is lower than the one obtained in the static adsorption experiments but is obtained after a much shorter time span, 30 min, compared with 4 h required by the static runs.

Finally, we embedded our gel in a dialysis membrane to treat a much larger volume of solution. To this aim, we charged a dialysis membrane (see the Materials and Methods section for details) with 1 g of the DBS-based gel in [bmpip][$NTf_2$], 3 wt %. The gel embedded in the dialysis membrane was then immersed in a beaker containing 20 mL of an aqueous solution of BPA. We measured the removal efficiency after 4, 24, and 48 h, obtaining RE % equal to 46, 64, and 85%, respectively.

Therefore, still, a good removal efficiency is maintained, although it requires a longer time.

To better assess the performance of our gels, we compared them with similar systems reported in the literature for the adsorption of BPA. These are reported in Table 5.

A comparison of the performance of our gels with the systems reported in Table 5 shows that our gels, albeit being simple systems, are competitive with most systems reported in the literature for BPA removal. In particular, among gel-based systems, our ILG exhibits higher adsorption capacity compared to polycyclodextrin-based hydrogels[24,25] (entries 1, 2, and 4) as well as compared with a hydrogel of graphene-silver phosphate composite[51] (entries 1 and 3). Furthermore, the DBS-based ILGs used in this work are also advantageous over an


https://doi.org/10.1021/acsmaterialsau.2c00066
ACS Mater. Au 2023, 3, 112−122

**Table 5. Adsorption Capacity of Our Gels and Other Systems Reported in the Literature to Adsorb BPA**

| entry | sorbent | time of contact (h) | $Q_{max}$ (mg/g) |
|---|---|---|---|
| 1 | DBS-based gel in [bmpip][$NTf_2$][a] | 4 | 214[b] |
| 2 | polycyclodextrin hydrogel[25] | 3 | 38 |
| 3 | $Ag_3PO_4$-graphene hydrogel[51] | 0.2 | 15 |
| 4 | polycyclodextrin hydrogel[24] | 2 | 21 |
| 5 | imidazolium-functionalized polymer gel[26] | 12 | 153 |
| 6 | xanthan gum-based hydrogel[23] | 4 | 458 |
| 7 | CTAB-modified graphite[52] | 0.5 | 125 |
| 8 | porphyrin-based porous organic polymer[53] | 2.5 | 653 |

[a]This work. [b]Highest $Q$ observed.

imidazolium-based polymer gel[26] (entries 1 and 5) in terms of either adsorption capacity or contact time. However, the performance of our gels is inferior to the one displayed by the xanthan gum-based gel described by Xie et al.[23] (entries 1 and 6), which, to the best of our knowledge, achieves the highest reported value for adsorption capacity of BPA for a gel-based system. Extending our comparison to systems not based on gels, we find that our ILGs show a higher adsorption ability of BPA with respect to a surfactant-modified graphite[52] (entries 1 and 7), while they are outperformed by a porphyrin-functionalized porous organic polymer,[53] which displays a 3 times higher adsorption efficiency in a shorter time of contact.

On the whole, these results clearly show that our gels are simple but effective sorbent systems for the removal of BPA. Furthermore, they are highly recyclable and can be embedded as a loading of columns and dialysis membranes for the treatment of flowing aqueous phases.

## CONCLUSIONS

In this work, we prepared and characterized supramolecular gels of DBS in aliphatic and aromatic ILs. All these gels showed good to high thermal stability, and gels obtained in aromatic ILs are featured by mechanically more resistant and flexible gel networks, compared with their aliphatic counterparts. The mechanical properties of the gels could be rationalized on the grounds of the different solvent−gelator interactions established in the three-dimensional network We applied these gels as sorbents for the removal of BPA from aqueous solutions, observing that all of them were capable of removing BPA almost entirely for the solutions, although the gels obtained in aliphatic ILs acted much faster than the ones obtained in aromatic ILs. Interestingly, the trend of the highest observed adsorption capacities allowed us to identify hydrogen bonds as the driving force in the adsorption process.

All gels could be reused several times without loss in performance and with no need for intermediate washing. In this respect, the best-performing one was the gel obtained in [bmpip][$NTf_2$] which maintained its removal efficiency higher than 90% over 37 cycles. Furthermore, we could recover 82% of BPA for the BPA-laden gel, after 41 adsorption runs, by letting it make contact for 5 min with ethylene glycol dimethyl ether. The same gel could be loaded in syringes for the sequential adsorption of BPA from flowing aqueous phases, observing a total RE % of 60% after 30 min. Finally, we embedded it in a dialysis membrane, to treat larger volumes of the solvent, finding a RE % of 85% after 48 h. A comparison of the performance of our gels with similar systems reported in the literature for the same purpose revealed that our gels are competitive with most systems considered in terms of adsorption capacity and time of action.

## ASSOCIATED CONTENT

### Supporting Information

The Supporting Information is available free of charge at https://pubs.acs.org/doi/10.1021/acsmaterialsau.2c00066.

Plots of rheology measurements, pictures of self-healing gels, tables of removal efficiency of gels in adsorption and recycle experiments, and tables of adsorption capacities as a function of equilibrium concentrations (PDF)

## AUTHOR INFORMATION


### Corresponding Author

**Francesca D'Anna** − *Dipartimento di Scienze Biologiche, Chimiche e Farmaceutiche, Università Degli Studi di Palermo, 90128 Palermo, Italia;* orcid.org/0000-0001-6171-8620; Email: francesca.danna@unipa.it

### Author

**Salvatore Marullo** − *Dipartimento di Scienze Biologiche, Chimiche e Farmaceutiche, Università Degli Studi di Palermo, 90128 Palermo, Italia;* orcid.org/0000-0001-9932-9823

Complete contact information is available at: https://pubs.acs.org/10.1021/acsmaterialsau.2c00066


### Author Contributions

CRediT: **Salvatore Marullo** data curation (equal), funding acquisition (equal), writing-original draft (equal); **Francesca D'Anna** conceptualization (equal), funding acquisition (equal), supervision (equal), writing-review & editing (equal).

### Notes

The authors declare no competing financial interest.

## ACKNOWLEDGMENTS

We thank the University of Palermo for financial support (FFR 2020-D'Anna and FFR 2020-Marullo).

## REFERENCES


(1) Daughton, C. G. Non-regulated water contaminants: emerging research. *Environ. Impact Assess. Rev.* **2004**, *24*, 711−732.

(2) Tang, Y.; Yin, M.; Yang, W.; Li, H.; Zhong, Y.; Mo, L.; Liang, Y.; Ma, X.; Sun, X. Emerging pollutants in water environment: Occurrence, monitoring, fate, and risk assessment. *Water Environ. Res.* **2019**, *91*, 984−991.

(3) Deblonde, T.; Cossu-Leguille, C.; Hartemann, P. Emerging pollutants in wastewater: A review of the literature. *Int. J. Hyg. Environ. Health* **2011**, *214*, 442−448.

(4) Guarnotta, V.; Amodei, R.; Frasca, F.; Aversa, A.; Giordano, C. Impact of Chemical Endocrine Disruptors and Hormone Modulators on the Endocrine System. *Int. J. Mol. Sci.* **2022**, *23*, 5710.

(5) Surana, D.; Gupta, J.; Sharma, S.; Kumar, S.; Ghosh, P. A review on advances in removal of endocrine disrupting compounds from aquatic matrices: Future perspectives on utilization of agri-waste based adsorbents. *Sci. Total Environ.* **2022**, *826*, 154129.

(6) Xing, J.; Zhang, S.; Zhang, M.; Hou, J. A critical review of presence, removal and potential impacts of endocrine disruptors bisphenol A. *Comp. Biochem. Physiol., Part C: Toxicol. Pharmacol.* **2022**, *254*, 109275.

(7) Geens, T.; Aerts, D.; Berthot, C.; Bourguignon, J.-P.; Goeyens, L.; Lecomte, P.; Maghuin-Rogister, G.; Pironnet, A.-M.; Pussemier, L.; Scippo, M.-L.; Van Loco, J.; Covaci, A. A review of dietary and non-dietary exposure to bisphenol-A. *Food Chem. Toxicol.* **2012**, *50*, 3725−3740.
(8) Zielińska, M.; Wojnowska-Baryła, I.; Cydzik-Kwiatkowska, A. *Bisphenol A Removal from Water and Wastewater*; Springer International Publishing AG, 2019; pp 29−75.
(9) Adegoke, K. A.; Olagunju, A. O.; Alagbada, T. C.; Alao, O. C.; Adesina, M. O.; Afolabi, I. C.; Adegoke, R. O.; Bello, O. S. Adsorptive Removal of Endocrine-Disrupting Chemicals from Aqueous Solutions: a Review. *Water, Air, Soil Pollut.* **2022**, *233*, 38.
(10) Bhatnagar, A.; Anastopoulos, I. Adsorptive removal of bisphenol A (BPA) from aqueous solution: A review. *Chemosphere* **2017**, *168*, 885−902.
(11) Sophia A, C.; Lima, E. C. Removal of emerging contaminants from the environment by adsorption. *Ecotoxicol. Environ. Saf.* **2018**, *150*, 1−17.
(12) Rakhym, A. B.; Seilkhanova, G. A.; Mastai, Y. Physicochemical evaluation of the effect of natural zeolite modification with didodecyldimethylammonium bromide on the adsorption of Bisphenol-A and Propranolol Hydrochloride. *Microporous Mesoporous Mater.* **2021**, *318*, 111020.
(13) Loffredo, E. Recent Advances on Innovative Materials from Biowaste Recycling for the Removal of Environmental Estrogens from Water and Soil. *Materials* **2022**, *15*, 1894.
(14) Mpatani, F. M.; Han, R.; Aryee, A. A.; Kani, A. N.; Li, Z.; Qu, L. Adsorption performance of modified agricultural waste materials for removal of emerging micro-contaminant bisphenol A: A comprehensive review. *Sci. Total Environ.* **2021**, *780*, 146629.
(15) Dehghani, M. H.; Ghadermazi, M.; Bhatnagar, A.; Sadighara, P.; Jahed-Khaniki, G.; Heibati, B.; McKay, G. Adsorptive removal of endocrine disrupting bisphenol A from aqueous solution using chitosan. *J. Environ. Chem. Eng.* **2016**, *4*, 2647−2655.
(16) dos Santos Cardoso, C.; Vitali, L. Chitosan Versus Chitosan-Vanillin Modified: An Evaluation of the Competitive Adsorption of Five Emerging Contaminants. *Water, Air, Soil Pollut.* **2021**, *232*, 179.
(17) El-sayed, M. E. A. Nanoadsorbents for water and wastewater remediation. *Sci. Total Environ.* **2020**, *739*, 139903.
(18) Khan, N. A.; Hasan, Z.; Jhung, S. H. Adsorptive removal of hazardous materials using metal-organic frameworks (MOFs): A review. *J. Hazard. Mater.* **2013**, *244−245*, 444−456.
(19) Zambare, R.; Song, X.; Bhuvana, S.; Antony Prince, J. S.; Nemade, P. Ultrafast Dye Removal Using Ionic Liquid-Graphene Oxide Sponge. *ACS Sustainable Chem. Eng.* **2017**, *5*, 6026−6035.
(20) Lim, J. Y. C.; Goh, S. S.; Liow, S. S.; Xue, K.; Loh, X. J. Molecular gel sorbent materials for environmental remediation and wastewater treatment. *J. Mater. Chem. A* **2019**, *7*, 18759−18791.
(21) Amabilino, D. B.; Smith, D. K.; Steed, J. W. Supramolecular materials. *Chem. Soc. Rev.* **2017**, *46*, 2404−2420.
(22) Draper, E. R.; Adams, D. J. Low-Molecular-Weight Gels: The State of the Art. *Chem* **2017**, *3*, 390−410.
(23) Chen, X.; Li, P.; Kang, Y.; Zeng, X.; Xie, Y.; Zhang, Y.; Wang, Y.; Xie, T. Preparation of temperature-sensitive Xanthan/NIPA hydrogel using citric acid as crosslinking agent for bisphenol A adsorption. *Carbohydr. Polym.* **2019**, *206*, 94−101.
(24) Gao, Y.; Guo, R.; Feng, Y.; Zhang, L.; Wang, C.; Song, J.; Jiao, T.; Zhou, J.; Peng, Q. Self-Assembled Hydrogels Based on Poly-Cyclodextrin and Poly-Azobenzene Compounds and Applications for Highly Efficient Removal of Bisphenol A and Methylene Blue. *ACS Omega* **2018**, *3*, 11663−11672.
(25) Kono, H.; Onishi, K.; Nakamura, T. Characterization and bisphenol A adsorption capacity of β-cyclodextrin-carboxymethylcellulose-based hydrogels. *Carbohydr. Polym.* **2013**, *98*, 784−792.
(26) Yang, Z.; Gan, C.; Feng, X.; Cai, G.; Zhang, J.; Ji, H. Imidazolium-functionalized stable gel materials for efficient adsorption of phenols from aqueous solutions. *Environ. Technol. Innovat.* **2020**, *17*, 100511.
(27) Billeci, F.; D'Anna, F.; Gunaratne, H. Q. N.; Plechkova, N. V.; Seddon, K. R. "Sweet" ionic liquid gels: materials for sweetening of fuels. *Green Chem.* **2018**, *20*, 4260−4276.
(28) Rizzo, C.; Misia, G.; Marullo, S.; Billeci, F.; D'Anna, F. Bio-based chitosan and cellulose ionic liquid gels: polymeric soft materials for the desulfurization of fuel. *Green Chem.* **2022**, *24*, 1318−1334.
(29) Rizzo, C.; Marullo, S.; Campodonico, P. R.; Pibiri, I.; Dintcheva, N. T.; Noto, R.; Millan, D.; D'Anna, F. Self-Sustaining Supramolecular Ionic Liquid Gels for Dye Adsorption. *ACS Sustainable Chem. Eng.* **2018**, *6*, 12453−12462.
(30) Rizzo, C.; Marullo, S.; D'Anna, F. Carbon-based ionic liquid gels: alternative adsorbents for pharmaceutically active compounds in wastewater. *Environ. Sci.: Nano* **2021**, *8*, 131−145.
(31) Okesola, B. O.; Vieira, V. M. P.; Cornwell, D. J.; Whitelaw, N. K.; Smith, D. K. 1,3:2,4-Dibenzylidene-d-sorbitol (DBS) and its derivatives - efficient, versatile and industrially-relevant low-molecular-weight gelators with over 100 years of history and a bright future. *Soft Matter* **2015**, *11*, 4768−4787.
(32) Ruiz-Olles, J.; Slavik, P.; Whitelaw, N. K.; Smith, D. K. Self-Assembled Gels Formed in Deep Eutectic Solvents: Supramolecular Eutectogels with High Ionic Conductivity. *Angew. Chem., Int. Ed.* **2019**, *58*, 4173−4178.
(33) Cornwell, D. J.; Okesola, B. O.; Smith, D. K. Hybrid polymer and low molecular weight gels - dynamic two-component soft materials with both responsive and robust nanoscale networks. *Soft Matter* **2013**, *9*, 8730−8736.
(34) Terech, P.; Pasquier, D.; Bordas, V.; Rossat, C. Rheological Properties and Structural Correlations in Molecular Organogels. *Langmuir* **2000**, *16*, 4485−4494.
(35) Takahashi, A.; Sakai, M.; Kato, T. Melting Temperature of Thermally Reversible Gel. VI. Effect of Branching on the Sol-Gel Transition of Polyethylene Gels. *Polym. J.* **1980**, *12*, 335−341.
(36) Marullo, S.; Meli, A.; Dintcheva, N. T.; Infurna, G.; Rizzo, C.; D'Anna, F. Environmentally Friendly Eutectogels Comprising l-a mino Acids and Deep Eutectic Solvents: Efficient Materials for Wastewater Treatment. *ChemPlusChem* **2020**, *85*, 301−311.
(37) Mukesh, C.; Upadhyay, K. K.; Devkar, R. V.; Chudasama, N. A.; Raol, G. G.; Prasad, K. Preparation of a Noncytotoxic Hemocompatible Ion Gel by Self-Polymerization of HEMA in a Green Deep Eutectic Solvent. *Macromol. Chem. Phys.* **2016**, *217*, 1899−1906.
(38) Itahara, T.; Tsuchida, T.; Morimoto, M. Solvent-driven swelling and shrinking of poly(NIPAM) gels crosslinked by tris-methacrylated phloroglucinol derivatives. *Polym. Chem.* **2010**, *1*, 1062−1066.
(39) Zu, Y.; Zhang, Y.; Zhao, X.; Shan, C.; Zu, S.; Wang, K.; Li, Y.; Ge, Y. Preparation and characterization of chitosan-polyvinyl alcohol blend hydrogels for the controlled release of nano-insulin. *Int. J. Biol. Macromol.* **2012**, *50*, 82−87.
(40) Huang, X.; Raghavan, S. R.; Terech, P.; Weiss, R. G. Distinct Kinetic Pathways Generate Organogel Networks with Contrasting Fractality and Thixotropic Properties. *J. Am. Chem. Soc.* **2006**, *128*, 15341−15352.
(41) Marullo, S.; Rizzo, C.; Dintcheva, N. T.; Giannici, F.; D'Anna, F. Ionic liquids gels: Soft materials for environmental remediation. *J. Colloid Interface Sci.* **2018**, *517*, 182−193.
(42) Crowhurst, L.; Mawdsley, P. R.; Perez-Arlandis, J. M.; Salter, P. A.; Welton, T. Solvent-solute interactions in ionic liquids. *Phys. Chem. Chem. Phys.* **2003**, *5*, 2790−2794.
(43) Dawn, A.; Kumari, H. Low Molecular Weight Supramolecular Gels Under Shear: Rheology as the Tool for Elucidating Structure-Function Correlation. *Chem.—Eur. J.* **2018**, *24*, 762−776.
(44) Rizzo, C.; Arrigo, R.; Dintcheva, N. T.; Gallo, G.; Giannici, F.; Noto, R.; Sutera, A.; Vitale, P.; D'Anna, F. Supramolecular Hydro- and Ionogels: A Study of Their Properties and Antibacterial Activity. *Chem.—Eur. J.* **2017**, *23*, 16297−16311.
(45) Rizzo, C.; Arcudi, F.; Đorđević, L.; Dintcheva, N. T.; Noto, R.; D'Anna, F.; Prato, M. Nitrogen-Doped Carbon Nanodots-Ionogels: Preparation, Characterization, and Radical Scavenging Activity. *ACS Nano* **2018**, *12*, 1296−1305.


https://doi.org/10.1021/acsmaterialsau.2c00066
*ACS Mater. Au* 2023, 3, 112−122

(46) Giles, C. H.; Smith, D.; Huitson, A. A general treatment and classification of the solute adsorption isotherm. I. Theoretical. *J. Colloid Interface Sci.* **1974**, *47*, 755−765.
(47) Jiang, N.; Erdős, M.; Moultos, O. A.; Shang, R.; Vlugt, T. J. H.; Heijman, S. G. J.; Rietveld, L. C. The adsorption mechanisms of organic micropollutants on high-silica zeolites causing S-shaped adsorption isotherms: An experimental and Monte Carlo simulation study. *Chem. Eng. J.* **2020**, *389*, 123968.
(48) Soares, S. F.; Rocha, M. J.; Ferro, M.; Amorim, C. O.; Amaral, J. S.; Trindade, T.; Daniel-da-Silva, A. L. Magnetic nanosorbents with siliceous hybrid shells of alginic acid and carrageenan for removal of ciprofloxacin. *Int. J. Biol. Macromol.* **2019**, *139*, 827−841.
(49) Chu, K. H. Fitting a little-known isotherm equation to S-shaped adsorption equilibrium data. *Sep. Purif. Technol.* **2021**, *259*, 118079.
(50) D'Anna, F.; La Marca, S.; Lo Meo, P.; Noto, R. A Study of the Influence of Ionic Liquids Properties on the Kemp Elimination Reaction. *Chem.—Eur. J.* **2009**, *15*, 7896−7902.
(51) Mu, C.; Zhang, Y.; Cui, W.; Liang, Y.; Zhu, Y. Removal of bisphenol A over a separation free 3D Ag 3 PO 4 -graphene hydrogel via an adsorption-photocatalysis synergy. *Appl. Catal., B* **2017**, *212*, 41−49.
(52) Wang, L.-C.; Ni, X.-j.; Cao, Y.-H.; Cao, G.-q. Adsorption behavior of bisphenol A on CTAB-modified graphite. *Appl. Surf. Sci.* **2018**, *428*, 165−170.
(53) Lee, M. Y.; Ahmed, I.; Yu, K.; Lee, C.-S.; Kang, K.-K.; Jang, M.-S.; Ahn, W.-S. Aqueous adsorption of bisphenol A over a porphyrinic porous organic polymer. *Chemosphere* **2021**, *265*, 129161.


https://doi.org/10.1021/acsmaterialsau.2c00066
*ACS Mater. Au* 2023, 3, 112−122